Semiclassical Mechanism for the Quantum Decay in Open Chaotic Systems

Daniel Waltner,[1] Martha Gutiérrez,[1] Arseni Goussev,[1,2] and Klaus Richter[1]
[1]*Institut für Theoretische Physik, Universität Regensburg, D-93040 Regensburg, Germany*
[2]*School of Mathematics, University of Bristol, University Walk, Bristol BS8 1TW, United Kingdom*
(Received 28 May 2008; published 23 October 2008)

We address the decay in open chaotic quantum systems and calculate semiclassical corrections to the classical exponential decay. We confirm random matrix predictions and, going beyond, calculate Ehrenfest time effects. To support our results we perform extensive numerical simulations. Within our approach we show that certain (previously unnoticed) pairs of interfering, correlated classical trajectories are of vital importance. They also provide the dynamical mechanism for related phenomena such as photoionization and photodissociation, for which we compute cross-section correlations. Moreover, these orbits allow us to establish a semiclassical version of the continuity equation.

DOI: 10.1103/PhysRevLett.101.174101 PACS numbers: 05.45.Mt, 03.65.Sq, 05.45.Pq

Besides their relevance to many areas of physics, open quantum systems play an outstanding role in gaining an improved understanding of the relation between classical and quantum physics [1]. For a closed quantum system the spatially integrated probability density

$$\rho(t) = \int_V d\mathbf{r}\,\psi(\mathbf{r}, t)\psi^*(\mathbf{r}, t) \tag{1}$$

of a wave function $\psi(\mathbf{r}, t)$ in the volume V is constant, i.e. $\rho(t) \equiv 1$. This fact is naturally retained when taking the classical limit in a semiclassical evaluation of Eq. (1), reflecting particle conservation in the quantum and classical limit. However, when opening up the system, $\rho(t)$, then representing the quantum survival probability, exhibits deviations from its classical counterpart $\rho_{\mathrm{cl}}(t)$; in other words, certain quantum properties of the closed system can be unveiled upon opening it.

For an open quantum system with a completely chaotic classical counterpart, i.e., fully hyperbolic dynamics, the classical survival probability is asymptotically $\rho_{\mathrm{cl}}(t) = \exp(-t/\tau_d)$, with classical dwell time τ_d. This has been observed in various disciplines, either directly, as in atom billiards [2,3], or indirectly in the spectral regime of Ericson fluctuations in electron [4] or microwave [5] cavities, and in atomic photoionization [6].

However, it was found numerically [7] and confirmed with supersymmetry techniques [8] that the difference between $\rho(t)$ and $\rho_{\mathrm{cl}}(t)$ becomes significant at times close to the quantum relaxation time $t^* = \sqrt{\tau_d t_H}$. In the semiclassical limit t^* is shorter than the Heisenberg time $t_H = 2\pi\hbar/\Delta$ (with Δ the mean level spacing). It was shown in Ref. [8] that $\rho(t)$ is a universal function depending only on τ_d and t_H in the random matrix theory (RMT) limit [9]. Though the leading quantum deviations from $\rho_{\mathrm{cl}}(t)$ were reproduced semiclassically for graphs [10], a general understanding of its dynamical origin is still lacking.

In this Letter we present a semiclassical calculation of $\rho(t)$ for $t < t^*$ for general, classically chaotic systems. It reveals the mechanism underlying the appearance of quantum corrections upon opening the system. In our calculation we go beyond the so-called diagonal approximation and evaluate contributions from correlated trajectory pairs [11]. This technique has been extended and applied to calculate various spectral [12,13] and scattering [14–19] properties of quantum chaotic systems. We find, however, that for calculating $\rho(t)$ a new class of correlated trajectory pairs, "one-leg-loops" (1ll), has to be considered along with the previously known loop diagrams. They prove particularly crucial for ensuring unitarity in problems involving semiclassical propagation along open trajectories inside a system and, moreover, allow one to semiclassically recover the continuity equation.

We present the dominant quantum corrections to $\rho_{\mathrm{cl}}(t)$ for systems with and without time reversal symmetry. Going beyond RMT, we calculate Ehrenfest time effects on $\rho(t)$ which are particularly pronounced in the time domain, compare with quantum simulations of billiard dynamics, and extend our approach to photoionization and photodissociation cross sections.

Semiclassical approach.—We consider $\rho(t)$, Eq. (1), for a two-dimensional system of area A and express $\psi(\mathbf{r}, t) = \int d\mathbf{r}' K(\mathbf{r}, \mathbf{r}'; t)\psi_0(\mathbf{r}')$ through the initial wave function $\psi_0(\mathbf{r}')$ and the time-dependent propagator $K(\mathbf{r}, \mathbf{r}'; t)$ that we approximate semiclassically by [20]

$$K_{\mathrm{sc}}(\mathbf{r}, \mathbf{r}'; t) = \frac{1}{2\pi i\hbar}\sum_{\tilde{\gamma}(\mathbf{r}'\to\mathbf{r},t)} D_{\tilde{\gamma}} e^{iS_{\tilde{\gamma}}/\hbar}. \tag{2}$$

Here $S_{\tilde{\gamma}} = S_{\tilde{\gamma}}(\mathbf{r}, \mathbf{r}'; t)$ is the classical action along the path $\tilde{\gamma}$ connecting $\mathbf{r}'$ and $\mathbf{r}$ in time t, and $D_{\tilde{\gamma}} = |\det(\partial^2 S_{\tilde{\gamma}}/\partial\mathbf{r}\partial\mathbf{r}')|^{1/2} e^{-i\pi\mu_{\tilde{\gamma}}/2}$ with Morse index $\mu_{\tilde{\gamma}}$.

The semiclassical survival probability, $\rho_{\mathrm{sc}}(t)$, obtained by expressing the time evolution of $\psi(\mathbf{r}, t)$ and $\psi^*(\mathbf{r}, t)$ in Eq. (1) through K_{sc}, Eq. (2), is given by three spatial integrals over a double sum over trajectories $\tilde{\gamma}$, $\tilde{\gamma}'$ starting at initial points $\mathbf{r}'$ and $\mathbf{r}''$, weighted by $\psi_0(\mathbf{r}')$ and $\psi_0^*(\mathbf{r}'')$, and ending at the same point $\mathbf{r}$ inside A. For simplicity of presentation we here assume ψ_0 to be spatially localized, so that contributions originate from points $\mathbf{r}'$ close to $\mathbf{r}''$ [21]; generalizations are given below. Introducing $\mathbf{r}_0 = (\mathbf{r}' + \mathbf{r}'')/2$ and $\mathbf{q} = (\mathbf{r}' - \mathbf{r}'')$, we replace the original paths $\bar{\gamma}$, $\bar{\gamma}'$, by nearby trajectories γ and γ' connecting $\mathbf{r}_0$ and $\mathbf{r}$ in time t. Then, upon expanding the action $S_{\bar{\gamma}}(\mathbf{r}, \mathbf{r}'; t) \simeq S_\gamma(\mathbf{r}, \mathbf{r}_0; t) - \mathbf{q}\mathbf{p}_0^\gamma/2$ (with $\mathbf{p}_0^\gamma$ the initial momentum of path γ) and $S_{\bar{\gamma}'}$ analogously, we obtain

$$\rho_{\mathrm{sc}}(t) = \frac{1}{(2\pi\hbar)^2} \int d\mathbf{r} d\mathbf{r}_0 d\mathbf{q}\, \psi_0\Big(\mathbf{r}_0 + \frac{\mathbf{q}}{2}\Big)\psi_0^*\Big(\mathbf{r}_0 - \frac{\mathbf{q}}{2}\Big) \times \sum_{\gamma,\gamma'(\mathbf{r}_0\to\mathbf{r},t)} D_\gamma D_{\gamma'}^* e^{(i/\hbar)[S_\gamma - S_{\gamma'} - (\mathbf{p}_0^\gamma + \mathbf{p}_0^{\gamma'})\mathbf{q}/2]}. \quad (3)$$

The double sums in Eq. (3) contain rapidly oscillating phases $(S_\gamma - S_{\gamma'})/\hbar$ which are assumed to vanish unless γ and γ' are correlated. The main, diagonal, contribution to ρ_{sc} arises from pairs $\gamma = \gamma'$ that, upon employing a sum rule [14], yield the classical decay $\rho_{\mathrm{cl}}(t) = \langle e^{-t/\tau_d}\rangle$. Here $\langle F\rangle = (2\pi\hbar)^{-2}\int d\mathbf{r}_0 d\mathbf{p}_0 F(\mathbf{r}_0, \mathbf{p}_0)\rho_W(\mathbf{r}_0, \mathbf{p}_0)$, where $\rho_W(\mathbf{r}_0, \mathbf{p}_0) = \int d\mathbf{q}\,\psi_0(\mathbf{r}_0 + \mathbf{q}/2)\psi_0^*(\mathbf{r}_0 - \mathbf{q}/2)e^{-(i/\hbar)\mathbf{q}\cdot\mathbf{p}_0}$ is the Wigner transform of the initial state and $\tau_d = \Omega(E)/2wp$, with $\Omega(E) = \int d\mathbf{r} d\mathbf{p}\,\delta(E - H(\mathbf{r}, \mathbf{p}))$ and w the size of the opening. For two-dimensional chaotic billiards $\tau_d(p) = m\pi A/wp$. For initial states with small energy dispersion $\rho_{\mathrm{cl}}(t) = e^{-t/\tau_d(p_0)}$. Our subsequent analysis is valid for times $\lambda t \gg 1$ where λ denotes the Lyapunov exponent. Furthermore we assume a small opening such that $\lambda\tau_d \gg 1$, while the number of channels $N = t_H/\tau_d$ is still large.

For systems with time reversal symmetry, leading-order quantum corrections to $\rho_{\mathrm{cl}}(t)$ arise from off-diagonal contributions to the double sum in Eq. (3), given by pairs of correlated orbits depicted as full and dashed line in Fig. 1(a), as in related semiclassical treatments [11,14–19]. The two orbits are exponentially close to each other along the two open "legs" and along the loop [14], but deviate in the intermediate encounter region [box in Fig. 1(a)]. Its length is $t_{\mathrm{enc}} = \lambda^{-1}\ln(c^2/|su|)$ [12], where c is a classical constant, and s and u are the stable and unstable coordinates in a Poincaré surface of section (PSS) in the encounter region. Such "two-leg-loops" (2ll) are based on orbit pairs with $S_\gamma - S_{\gamma'} = su$ and a density $w_{2\mathrm{ll}}(s, u, t) = [t - 2t_{\mathrm{enc}}(s, u)]^2/[2\Omega(E)t_{\mathrm{enc}}(s, u)]$ [19]. Invoking the sum rule, the double sum in Eq. (3) is replaced by $\int du \int ds e^{(-t+t_{\mathrm{enc}})/\tau_d} w_{2\mathrm{ll}}(s, u, t)e^{(i/\hbar)su}$. Here $e^{t_{\mathrm{enc}}/\tau_d}$ accounts for the fact that if the first encounter stretch is inside A the second must also be inside A. This gives the 2ll contribution [Fig. 1(a)] to $\rho(t)$ (for $t < t^*$):

$$\rho_{2\mathrm{ll}}(t) = e^{-t/\tau_d}\Big(-2\frac{t}{t_H} + \frac{t^2}{2\tau_d t_H}\Big). \quad (4)$$

The linear term in Eq. (4) violates unitarity, since it does not vanish upon closing the system, i.e., as $\tau_d \to \infty$. This is cured by considering a *new type of diagrams*. These orbit pairs, to which we refer as one-leg-loops, are characterized by an initial or final point inside the encounter region

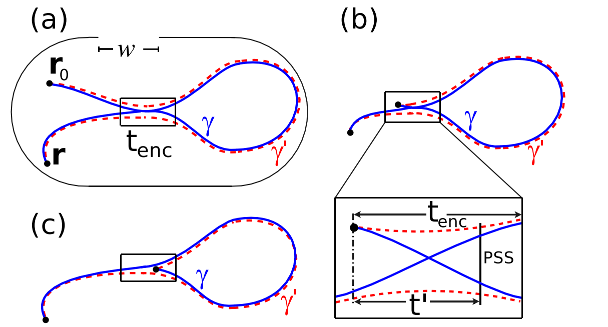

FIG. 1 (color online). Pairs of correlated classical trajectories γ (full line) and γ' (dashed) generating the leading quantum corrections to the classical decay probability. While in panel (a) the encounter region (box) connects a loop with two legs, the paths begin or end inside the encounter region ("one-leg-loops") in (b) with and in (c) without a self-crossing in configuration space. The zoom into the encounter region in (b) depicts the position of the Poincaré surface of section used.

[Figs. 1(b) and 1(c)]. They are relevant for open orbits starting or ending *inside A* and hence have not arisen in conductance treatments based on lead-connecting paths, since at an opening the exit of one encounter stretch implies the exit of the other one.

For their evaluation consider the time t' between the initial or final point of the trajectory and the PSS, defined in the zoom into Fig. 1(b). Then $t_{\mathrm{enc}}(t', u) = t' + \lambda^{-1}\ln(c/|u|)$ and $S_\gamma - S_{\gamma'} = su$ for any position of the PSS. The density of encounters is $w_{1\mathrm{ll}}(s, u, t) = 2\int_0^{\lambda^{-1}\ln(c/|s|)} dt'[t - 2t_{\mathrm{enc}}(t', u)]/[\Omega(E)t_{\mathrm{enc}}(t', u)]$, where the prefactor 2 accounts for the two cases of beginning or ending in an encounter region. We evaluate this contribution by modifying $\rho_{\mathrm{cl}}(t)$ by $e^{t_{\mathrm{enc}}/\tau_d}$ as before and integrating over s, u and t'. To this end we substitute [17] $t'' = t' + \lambda^{-1}\ln(c/|u|)$, $\sigma = c/u$ and $x = su/c^2$, with integration domains $-1 < x < 1$, $1 < \sigma < e^{\lambda t''}$ and $0 < t'' < \lambda^{-1}\ln(1/|x|)$. Note that the limits for t' include the case when the paths do not have a self-crossing in configuration space [Fig. 1(c)]. The integration yields

$$\rho_{1\mathrm{ll}}(t) = 2\frac{t}{t_H}e^{-t/\tau_d}. \quad (5)$$

It precisely cancels the linear term in $\rho_{2\mathrm{ll}}$, Eq. (4), i.e., $\rho_{2\mathrm{ll}}(t) + \rho_{1\mathrm{ll}}(t) = e^{-t/\tau_d}t^2/(2\tau_d t_H)$, recovering unitarity.

The next-order quantum corrections are obtained by calculating [22] 1ll and 2ll contributions of diagrams such as discussed in [12]. Together with Eqs. (4) and (5), this yields for systems with time reversal symmetry

$$\rho_{\mathrm{sc}}(t) \simeq e^{-t/\tau_d}\Big(1 + \frac{t^2}{2\tau_d t_H} - \frac{t^3}{3\tau_d t_H^2} + \frac{5t^4}{24\tau_d^2 t_H^2}\Big). \quad (6)$$

The term quadratic in t represents the weak-localization-type enhancement of the quantum survival probability. The expansion in Eq. (6) agrees with RMT [8].

For systems without time reversal symmetry the calculation of the relevant one- and two-leg-loops gives, again in accordance with RMT [8],

$$\rho_{\rm sc}(t) \simeq e^{-t/\tau_d}\left(1 + \frac{t^4}{24\tau_d^2 t_H^2}\right). \tag{7}$$

We finally note that our restriction to localized initial states can be lifted and the results generalized to arbitrary initial states by considering an additional local time average of $\rho(t)$. This amounts to selecting in Eq. (3) trajectory pairs $\bar\gamma$, $\bar\gamma'$ starting at adjacent points [22].

Continuity equation.—It is instructive to reformulate the decay problem in terms of paths crossing the opening. To this end we consider the integral version of the continuity equation, $\partial\rho(\mathbf{r}, t)/\partial t + \nabla\cdot\mathbf{j}(\mathbf{r}, t) = 0$, namely

$$\frac{\partial}{\partial t}\rho(t) = -\int_S \mathbf{j}(\mathbf{r}, t)\cdot\hat n_x dx, \tag{8}$$

where S is the cross section of the opening with a normal vector $\hat n_x$. In Eq. (8), the current density $\mathbf{j}(\mathbf{r}, t) = (1/m)\mathrm{Re}[(\hbar/i)\psi^*(\mathbf{r}, t)\nabla\psi(\mathbf{r}, t)]$ can be semiclassically expressed through Eq. (2) in terms of orbit pairs connecting points inside A with the opening. In the diagonal approximation we obtain $\int_S \mathbf{j}_{\rm diag}\cdot\hat n_x dx = e^{-t/\tau_d}/\tau_d$, consistent with $\rho_{\rm cl}(t)$. Loop contributions are calculated analogously to those of $\rho_{\rm sc}$ from Eq. (3), giving

$$\int_S(\mathbf{j}_{2\rm ll} + \mathbf{j}_{1\rm ll})\cdot\hat n_x dx = e^{-t/\tau_d}\frac{t^2 - 2t\tau_d}{2\tau_d^2 t_H}. \tag{9}$$

Time integration of Eq. (8) leads to $\rho_{2\rm ll}(t) + \rho_{1\rm ll}(t) = e^{-t/\tau_d}t^2/(2\tau_d t_H)$, consistent with Eq. (6). The 1ll contributions enter into Eq. (9) with half the weight, since 1ll's with a short leg (encounter box) at the opening must be excluded. These "missing" paths assure the correct form of quantum deviations from $\rho_{\rm cl}(t)$.

Higher 2ll and 1ll corrections to $\mathbf{j}$ lead to Eqs. (6) and (7). We conclude that both, 2ll *and* 1ll contributions to $\mathbf{j}$ are essential to achieve a unitary flow and thereby to establish a semiclassical version of the continuity equation.

Ehrenfest time effects.—The Ehrenfest time τ_E [23] separates the evolution of wave packets following essentially the classical dynamics from longer time scales dominated by wave interference. While τ_E effects have been mainly considered for stationary processes involving time integration [15–18,24,25], signatures of τ_E should appear most directly in the time domain [13,26], i.e., for $\rho(t)$. Here we semiclassically compute the τ_E dependence of the weak-localization correction to $\rho(t)$ in Eq. (6). To this end we distinguish between $\tau_E^c = \lambda^{-1}\ln(\mathcal{L}/\lambda_B)$, where $\mathcal{L}$ is the typical system size and λ_B the de Broglie wavelength, and $\tau_E^o = \lambda^{-1}\ln[w^2/(\mathcal{L}\lambda_B)]$, related to the width w of the opening [18]. As before we consider that the densities $w_{2\rm ll,1ll}(s, u, t)$ contain the Heaviside function $\theta(t - 2t_{\rm enc})$ (negligible for $\tau_E^{o,c} \ll \tau_d$) assuring that the time required to form a 1ll or 2ll is larger than $2t_{\rm enc}$. Our calculation gives (for $\tau_E^{o,c}\lambda \gg 1$ with $2\tau_E^e = \tau_E^o + \tau_E^c$)

$$\rho_{2\rm ll}(t) + \rho_{1\rm ll}(t) = e^{-(t-\tau_E^o)/\tau_d}\frac{(t - 2\tau_E^e)^2}{2\tau_d t_H}\theta(t - 2\tau_E^e). \tag{10}$$

Numerical simulation.—The leading-order quantum corrections in Eqs. (6) and (7) were confirmed by numerical simulations for graphs [10]. Here we compare our semiclassical predictions with quantum calculations of $\rho(t)$ based on the numerical propagation of Gaussian wave packets inside a billiard, a setup much closer to experiment. We chose the desymmetrized diamond billiard (inset Fig. 2) [27] that is classically chaotic ($\lambda^{-1} \simeq 3\tau_f$, with τ_f the mean free flight time). Its opening w corresponds to $N = 10$ channels and $\tau_d \simeq 15\tau_f$ for $\lambda_B = 3$. For the simulations we reach $t_H = 10.6\tau_d$ implying $t^* = 3.3\tau_d$, $\tau_E^o \simeq 0.17\tau_d$, and $\tau_E^c \simeq 0.55\tau_d$ (with $\mathcal{L} = \sqrt{A}$).

In the upper inset of Fig. 2 we compare the decay $\rho_{\rm qm}^{\rm sim}(t)$ (red full line) for a representative wave packet simulation with the corresponding classical, $\rho_{\rm cl}^{\rm sim}(t)$ (dashed line), obtained from an ensemble of trajectories with the same phase space distribution as the Wigner function of the initial quantum state. $\rho_{\rm cl}^{\rm sim}(t)$ merges into the exponential decay $\exp(-t/\tau_d)$, and $\rho_{\rm qm}^{\rm sim}(t)$ coincides with $\rho_{\rm cl}^{\rm sim}(t)$ up to scales of t^*. For a detailed analysis of the quantum deviations we consider the ratio $R(t) \equiv [\rho_{\rm qm}^{\rm sim}(t) - \rho_{\rm cl}^{\rm sim}(t)]/\rho_{\rm cl}^{\rm sim}(t)$. The red dots in Fig. 2 represent an average of $R(t)$ over 27 different opening positions and initial momentum directions. The dashed and full curve depict the semiclassical results based on the quadratic term in Eq. (6)

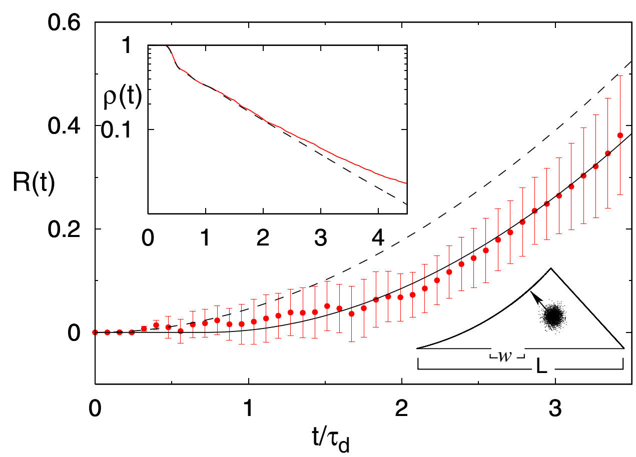

FIG. 2 (color online). Averaged ratio $R(t)$ between numerical quantum mechanical decay $\rho_{\rm qm}^{\rm sim}(t)$ and classical decay $\rho_{\rm cl}^{\rm sim}(t)$ (red dots, the bars correspond to the standard deviation after averaging, see text) compared with corresponding semiclassical predictions based on the quadratic term in Eq. (6) (dashed line) and Eq. (10) (full line). Upper inset: $\rho_{\rm qm}^{\rm sim}(t)$ (red full line) and $\rho_{\rm cl}^{\rm sim}(t)$ (dashed) for the wave packet shown in the lower inset. Lower inset: Desymmetrized diamond billiard, defined as the fundamental domain of the area confined by four intersecting disks of radius R centered at the vertices of a square of length $2L$ ($L = 100$, $R = 131$) with opening $w = 16$. The initial Gaussian wave packet shown is of size $\sigma = 3$ and $\lambda_B = 3$. The arrow indicates the momentum direction.

(dominant for the t/τ_d range displayed) and on Eq. (10). The overall agreement of the numerical data with the full curve indicates τ_E signatures. We note, however, that we cannot rule out other nonuniversal effects (e.g., due to scars [9], short orbits, diffraction, or fluctuations of the effective τ_d [7]) that may also yield time shifts. Furthermore the individual numerical traces $R(t)$ exhibit strong fluctuations (reflected in a large standard deviation in Fig. 2). A numerical confirmation of the $\log(1/\hbar)$ dependence of τ_E seems to date impossible for billiards.

Photoionization and photodissociation cross sections.— Related to the decay problem are photoabsorption processes where a molecule [28] (or correspondingly an atom) is excited into a classically chaotic, subsequently decaying resonant state. In dipole approximation, the photodissociation cross section of the molecule excited from the ground state $|g\rangle$ is $\sigma(\epsilon) = \mathrm{Im}\mathrm{Tr}\{\hat{A}G(\epsilon)\}$, where $G(\epsilon)$ is the retarded molecule Green function, $\hat{A} = [\epsilon/(c\hbar\epsilon_0)]|\phi\rangle\langle\phi|$ and $|\phi\rangle = D|g\rangle$, with $D = \mathbf{d}\cdot\hat{\mathbf{e}}$ the projection of the dipole moment on the light polarization $\hat{\mathbf{e}}$. The two-point correlation function of $\sigma(\epsilon)$ is defined as

$$C(\omega) = \langle\sigma(\epsilon + \omega\Delta/2)\sigma(\epsilon - \omega\Delta/2)\rangle_\epsilon/\langle\sigma(\epsilon)\rangle_\epsilon^2 - 1. \tag{11}$$

Here $\langle\sigma(\epsilon)\rangle_\epsilon \approx \pi(2\pi\hbar)^{-2}\int d\mathbf{r}d\mathbf{p}A_W(\mathbf{r},\mathbf{p})\delta(\epsilon - H(\mathbf{r},\mathbf{p}))$ semiclassically, with Wigner transform A_W of $\hat{A}$. Previous semiclassical treatments of $C(\omega)$ [29,30] were limited to the diagonal approximation. To compute off-diagonal (loop) terms we consider $Z(\tau) = \int_{-\infty}^{\infty} d\omega e^{2\pi i\omega\tau}C(\omega)$ with $\tau = t/t_H$. Semiclassically, Z_{sc} is again given by a double sum over orbits with different initial and final points in an open system with N decay channels. Because of rapidly oscillating phases from the action differences, only two possible configurations of those points contribute [29]: (i) orbits in a sum similar to Eq. (3) leading to a contribution as for $\rho_{\mathrm{sc}}(t)$; (ii) trajectories in the vicinity of a periodic orbit. Expanding around it, as in [30], leads to the spectral form factor $K_{\mathrm{sc}}^{\mathrm{open}}(\tau)$ of an open system. From (i) and (ii) we have $Z_{\mathrm{sc}}(\tau) = K_{\mathrm{sc}}^{\mathrm{open}}(\tau) + 2\rho_{\mathrm{sc}}(\tau)$ for the time reversal case. Up to second order in $\tau > 0$ we find $K_{\mathrm{sc}}^{\mathrm{open}}(\tau) = e^{-N\tau}(2\tau - 2\tau^2)$ [31] and $\rho_{\mathrm{sc}}(\tau) = e^{-N\tau}(1 + N\tau^2/2)$ [Eq. (6)]. Thereby $Z_{\mathrm{sc}}(\tau) = e^{-N\tau}[2 + 2\tau + (N-2)\tau^2]$, confirming a conjecture of [32]. Its inverse Fourier transform yields the two-point correlation (with $\Gamma = 2\pi\omega/N$)

$$C_{\mathrm{sc}}(\Gamma) = \frac{4}{N}\frac{1}{1+\Gamma^2}\left[1 + \frac{1}{N}\frac{1-\Gamma^2}{1+\Gamma^2} + \frac{N-2}{N^2}\frac{1-3\Gamma^2}{(1+\Gamma^2)^2}\right]. \tag{12}$$

The first two diagonal terms agree with [29]; the third term represents the leading quantum correction.

To conclude, we presented a general semiclassical approach to the problems of quantum decay and photo cross-section statistics in open chaotic quantum systems.

We thank İ. Adagideli, J. Kuipers, and C. Petitjean for useful discussions and for a critical reading of the manuscript. We acknowledge funding by DFG under GRK 638 and the A. von Humboldt Foundation (A. G.).

[1] For a recent account of quantum chaotic scattering see, e.g., Special Issue on trends in quantum chaotic scattering [J. Phys. A **38**, 10 433 (2005)].
[2] V. Milner *et al.*, Phys. Rev. Lett. **86**, 1514 (2001).
[3] N. Friedman *et al.*, Phys. Rev. Lett. **86**, 1518 (2001).
[4] C. M. Marcus *et al.*, Phys. Rev. Lett. **69**, 506 (1992).
[5] E. Doron, U. Smilansky, and A. Frenkel, Phys. Rev. Lett. **65**, 3072 (1990).
[6] G. Stania and H. Walther, Phys. Rev. Lett. **95**, 194101 (2005).
[7] G. Casati, G. Maspero, and D. L. Shepelyansky, Phys. Rev. E **56**, R6233 (1997).
[8] K. M. Frahm, Phys. Rev. E **56**, R6237 (1997); D. V. Savin and V. V. Sokolov, Phys. Rev. E **56**, R4911 (1997); D. V. Savin and H.-J. Sommers, Phys. Rev. E **68**, 036211 (2003).
[9] For a comprehensive analysis of (scar) effects beyond RMT, see L. Kaplan, Phys. Rev. E **59**, 5325 (1999).
[10] M. Puhlmann *et al.*, Europhys. Lett. **69**, 313 (2005).
[11] M. Sieber and K. Richter, Phys. Scr. **T90**, 128 (2001); M. Sieber, J. Phys. A **35**, L613 (2002).
[12] S. Müller *et al.*, Phys. Rev. Lett. **93**, 014103 (2004).
[13] P. W. Brouwer, S. Rahav, and C. Tian, Phys. Rev. E **74**, 066208 (2006).
[14] K. Richter and M. Sieber, Phys. Rev. Lett. **89**, 206801 (2002).
[15] İ. Adagideli, Phys. Rev. B **68**, 233308 (2003).
[16] S. Rahav and P. W. Brouwer, Phys. Rev. Lett. **96**, 196804 (2006).
[17] P. W. Brouwer and S. Rahav, Phys. Rev. B **74**, 075322 (2006).
[18] Ph. Jacquod and R. S. Whitney, Phys. Rev. B **73**, 195115 (2006).
[19] S. Heusler *et al.*, Phys. Rev. Lett. **96**, 066804 (2006).
[20] M. Gutzwiller, *Chaos in Classical and Quantum Mechanics* (Springer, New York, 1990).
[21] For a detailed analysis, see A. Goussev *et al.*, New J. Phys. **10**, 093010 (2008).
[22] M. Gutiérrez *et al.* (to be published).
[23] B. V. Chirikov, F. M. Izrailev, and D. L. Shepelyansky, Sov. Sci. Rev. Sect. C **2**, 209 (1981).
[24] I. L. Aleiner and A. I. Larkin, Phys. Rev. B **54**, 14 423 (1996).
[25] O. Yevtushenko *et al.*, Phys. Rev. Lett. **84**, 542 (2000).
[26] H. Schomerus and J. Tworzydło, Phys. Rev. Lett. **93**, 154102 (2004); H. Schomerus and Ph. Jacquod, J. Phys. A **38**, 10 663 (2005).
[27] For more details of the simulations, see A. Goussev and K. Richter, Phys. Rev. E **75**, 015201 (2007).
[28] R. Schinke, *Photodissociation Dynamics* (Cambridge University Press, Cambridge, U.K., 1993).
[29] O. Agam, Phys. Rev. E **61**, 1285 (2000).
[30] B. Eckhardt, S. Fishman, and I. Varga, Phys. Rev. E **62**, 7867 (2000).
[31] J. Kuipers and M. Sieber, Nonlinearity **20**, 909 (2007).
[32] T. Gorin, J. Phys. A **38**, 10 805 (2005).